Available online at www.sciencedirect.com
SCIENCE DIRECT®
Journal of Chromatography A, 1051 (2004) 141–146
JOURNAL OF CHROMATOGRAPHY A
www.elsevier.com/locate/chroma

Size-based continuous-flow directional control of DNA with a nano-pillar anisotropic array

Wataru Hattori*, Hiroko Someya, Masakazu Baba, Hisao Kawaura

Fundamental and Environmental Research Laboratories, NEC Corporation, 34 Miyukigaoka, Tsukuba, Ibaraki, Japan

Abstract

A size-based pre-fractionation chip applicable for enrichment of macromolecules in biological samples is proposed. In this chip, a fractionation unit with a nano-pillar anisotropic array, which functions as sieve meshes, is installed at a bi-forked junction. The mesh sizes are close to the diameters of macromolecules and vary according to the direction to the main and branch exit channels. This fractionation unit provides continuous-flow fractionation without both the dilution of samples and the limitations with the sample loading volume. Additionally, the small channel-volume, which is characteristic of chip-based systems, can reduce sample loss. Using nanometer-scale fabrication technology, we fabricated the chips and demonstrated the flow direction control of DNA molecules.

Keywords: Size-based pre-fractionation chip; Nano-pillar anisotropic array; Continuous-flow fractionation

1. Introduction

The demand for high-sensitivity analyses of biological samples has made pre-fractionation strategies more attractive. Two-dimensional gel electrophoresis (2-DE) is the most widely used in proteome studies, where proteins are separated and visualized on a two-dimensional map with a few thousands of spots according to their isoelectric points and their molecular weights. Despite the resolution, it has been estimated that numerous kinds of low abundant proteins cannot be visualized due to deficiencies with dynamic range and resolution [1–3]. Consequently, the concentration of low abundant proteins prior to 2-DE continues to be important and needs to be addressed to overcome these limitations. These days, pre-fractionation for sample enrichment is considered to be one of the most promising approaches to achieving this concentration.

Pre-fractionation based on size in relation to molecular mass is one of the most fundamental approaches because of the universality of its usage. Conventional size-based pre-fractionation using a size-exclusion chromatographic column, however, is rarely used because this results in considerable penalties in sample recovery. Neither lost samples due to proteins adhering to porous beads in the columns nor those lost in the post-concentration step of diluted sample fractions can be ignored [1].

In recent years, nano- or micro-fabricated separation chip technology has been on the increase [4–6]. Baba et al. reported two types (molecular sieving and size-exclusion chromatography) of size-based DNA band separation using nano-structured matrices fabricated in micro-channels on silicon chips [5]. Lately, molecular sieving type DNA band separation was confirmed by Kaji et al. using a quarts nano-pillar chip [6]. The small amount of sample loss with these chip-based systems is one of their major advantages due to their small channel-volume. The batch mode operation according to the cross injection technique [4], however, deteriorates the sample usage rate. Additionally, this small channel-volume and the batch mode operation limit the loading volume of samples.

Chou et al. reported on a continuous-flow size-based fractionation chip [7,8]. This continuous-flow operation resolved the limitations with small loading volume and allowed this chip to be applicable for pre-fractionation. To achieve continuous-flow operation, the asymmetrical micrometer-

* Corresponding author. Fax: +81 29 856 6139.
E-mail address: w-hattori@bl.jp.nec.com (W. Hattori).

0021-9673/$ – see front matter © 2004 Elsevier B.V. All rights reserved.
doi:10.1016/j.chroma.2004.08.045

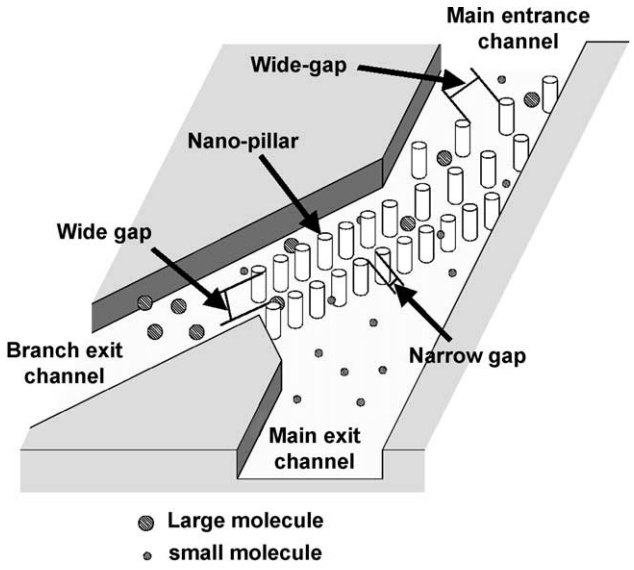

Fig. 1. Outline of continuous-flow fractionation unit with two-dimensional nano-pillar anisotropic array. This unit is located in bi-forked junction with branch and main channel. Large molecules cannot pass through narrow gap and therefore flow in branch exit channel, while small molecules predominantly flow into the main exit channel.

scale obstacles (1.5 μm × 6.0 μm in measure) were fabricated in the channel by exploiting the design flexibility afforded by semiconductor device fabrication technology. This asymmetrical shape induced micrometer-scale anisotropic diffusion lengths caused by Brownian motion, which varied according to the sizes of macromolecules and provided continuous-flow operation.

Using further advanced nanometer-scale fabrication technology approaching the macromolecular size, we successfully demonstrated sieving type continuous-flow fractionation unit applicable for size-based pre-fractionation chip. This chip had a fractionation unit with a nano-pillar anisotropic array, which functioned as sieve meshes, is arranged at a bi-forked junction. The mesh sizes were close to the diameters of macromolecules and varied according to the direction to the main or branch channels. This report first describes the conceptual design and the operation of a proposed pre-fractionation chip. We then describe the fabrication of chips with continuous-flow fractionation units and demonstrate that they can control the flow direction of electrophoretic DNA molecules according to their respective sizes.

2. Conceptual chip design and operating principles

The basic building block of the proposed pre-fractionation chip is its bi-forked junction with its branch and main channels, as shown in Fig. 1. A continuous-flow fractionation unit with a two-dimensional anisotropic array of nano-pillars is installed at the junction. The gap between all nano-pillars opening to the branch exit channel is wide enough for macromolecules of various sizes to pass through. The gap opening to the main exit channel is monotonously varied from the junction entrance to the exit. The gap near the entrance is also wide to allow macromolecules to enter easily. However, the gap near the exit is as narrow as the diameters of the macromolecules, functioning as a sieve mesh. This two-dimensional array of gaps is intended to prevent macromolecules from gathering in a line on mesh with specific gap widths, and from blocking up narrow gaps.

When different-sized macromolecules flow in from the main entrance channel, this fractionation unit operates as follows. Large molecules, which cannot pass through the narrow gap to the main exit channel, are forced to flow in the branch exit channel through the wide gap. Small molecules, on the other hand, which can pass through the narrow gap, can flow in both the main and branch exit channels. Then, the driving force to the main exit channel is stronger than that to the branch exit channel. For example, when pumps drive the flow, the flow rate to the main exit channel is higher than that to the branch exit channel. Alternatively, when the macromolecules are electrophoresed, the electric field to the main exit channel is higher than that to the branch exit channel. As a result, small macromolecules flow predominantly into the main exit channel, and flow to the branch exit channel is curbed.

This can be done continuously in contrast to the batch operation in a size-exclusion chromatographic column. Additionally, because samples do not have to be diluted with fractionation, no sample loss occurs due to the post-concentration step. Furthermore, because a small channel-volume can also be achieved with this pre-fractionation chip, the sample loss due to their adhering to channel walls can be reduced. Consequently, this pre-fractionation chip has a prospective feature of low sample loss.

The operating principle is based on sieving through narrow gaps, whose widths are comparable to the diameters of macromolecules. In contrast to the diffusion principle with Chou et al.'s continuous-flow fractionation chip, this sieving principle does not include the spreading factor in fractional resolution due to binominal statistics [7]. Therefore, small amounts of cross contamination between fractionated samples can be expected with our chip in comparison with Chou et al.'s.

3. Experimental

3.1. Fabrication process and chip layout

We fabricated demonstration chips to prove the effectiveness of conceptual chip design and its operating principles. We used the nanometer-scale fabrication process in Fig. 2 to achieve mesh sizes between nano-pillars that were as close to the diameters of macromolecules as possible.

We first spin-coated a 80-nm-thick calixarene negative resist [5,9] on a silicon wafer with 40-nm-thick silicon dioxide

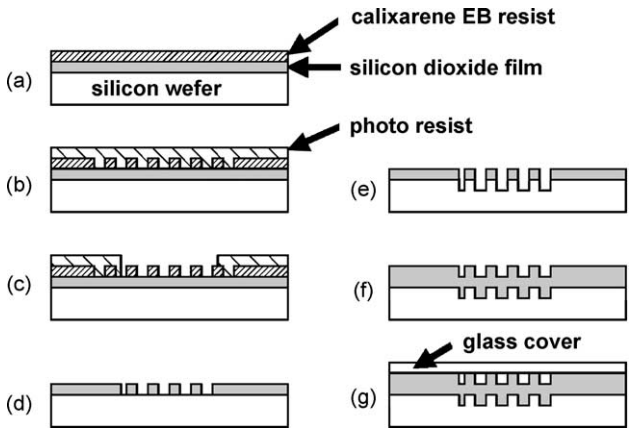

Fig. 2. Cross-sectional views illustrate the nanometer-scale fabrication process. (a) Eighty-nanometers-thick calixarene negative resist on silicon wafer with 40-nm-thick silicon dioxide film. This calixarene resist is patterned with electron-beam lithography. (b) 1.8-μm-thick photoresist on wafer with calixarene resist pattern. (c) Photo resist is patterned by photolithography and channel pattern is formed. (d) Transfer of pattern to silicon dioxide film by dry-etching. (e) Three-hundred and sixty-nanometers-deep silicon dry-etching using silicon dioxide mask. (f) Two-hundred and forty-nanometers-thick silicon dioxide film is grown by thermal oxidization. (g) Glass cover anodically bonded to chip.

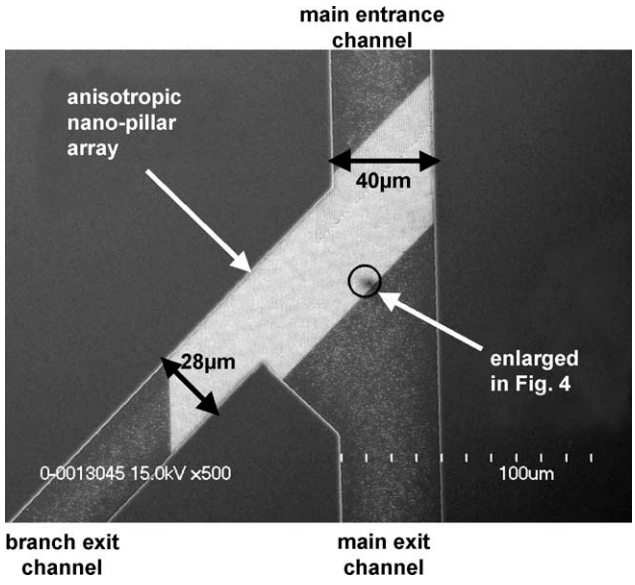

Fig. 3. Top-view scanning electron micrograph of bi-forked channel layout. This junction functions as continuous-flow fractionation unit. 28-μm-wide branch channel leaves at angle of 45° from straight 40-μm-wide main channel. White part in junction is nano-pillar anisotropic array.

film, as outlined in Fig. 2a. We then formed nano-pillar resist patterns with electron-beam lithography, which enabled us to lay out their positions in increments of 1.25 nm. This chip could fractionate proteins due to this fine resolution, which are commonly analyzed with 2-DE with molecular masses ranging from almost 10 000 to 100 000 into almost 10 fractions according to their corresponding diameters ranging from 5 to 15 nm.

We next spin-coated 1.8-μm-thick positive photoresist onto the wafer with the calixarene resist pattern, and formed the channel pattern with photolithography. The resist masks were then transferred to the silicon dioxide film pattern through dry-etching. The silicon channels with 360-nm-tall nano-pillars were fabricated by dry-etching with this silicon dioxide mask as described in Fig. 2e.

After the patterning, 240-nm-thick thermally oxidized silicon dioxide film was grown on the silicon wafer, which provided electrical isolation. This thermal oxidization process also reduced limitations with pattern resolution in electron-beam lithography. The expansion in volume due to thermal oxidization caused the diameters of the nano-pillars to increase and easily enabled to fabricate narrower gaps to be fabricated between nano-pillars than those between the calixarene resist patterns.

After the wafer was diced into chips, each chip was anodically bonded to a glass cover on which glass reservoirs were glued at the end of each channel.

We fabricated three chips (chips A, B, and C) according to this process with different sieve meshes. These chips had a bi-forked channel layout as can be seen in Fig. 3. The 28-μm-wide branch channel leaves the 40-μm-wide straight main channel at an angle of 45°. The two-dimensional anisotropic array of nano-pillars was arranged at the junction. Fig. 4 has enlarged scanning electron micrographs of arrays at the junction exit of the main exit channel. The intervals between nano-pillars were varied with directions and this layout constitutes anisotropy in the arrays. The constant interval between nano-pillars in the direction of the main exit channel was 500 nm in each chip. The intervals between those in the direction of the branch exit channel were monotonously decreased from 500 nm at the junction entrance of the main channel to 177, 194, and 212 nm at the junction exit of respective chips A, B, and C. The gap widths at the junction exits opening to the main exit channels varied in respective chips according to this layout. Fig. 5 has an oblique-perspective view of the nano-pillar array in chip B observed downward at an angle of 45°. The maximum diameters of the particles, which could pass through the gaps opening to the main exit channels, were estimated to be 32, 52, and 70 nm for respective chips A, B, and C from this view.

3.2. Electrophoretic conditions

The whole channel was initially filled and treated for several hours with 1% 2-methacryloxy ethyl phosphorylcholine diluted with a 1× Tris–borate etylenediamine tetraacetic acid (TBE) buffer for the dynamic coating to suppress electroosmotic flow [5,10].

We adopted DNA molecules as macromolecules and electrophoresis as the driving method to demonstrate chip operation. The dependence of DNA size on the direction of electrophoretic flow was observed through a fluorescent microscope. DNA fluorescently stained with YOYO-1 was introduced one size at a time through the reservoir at the inlet

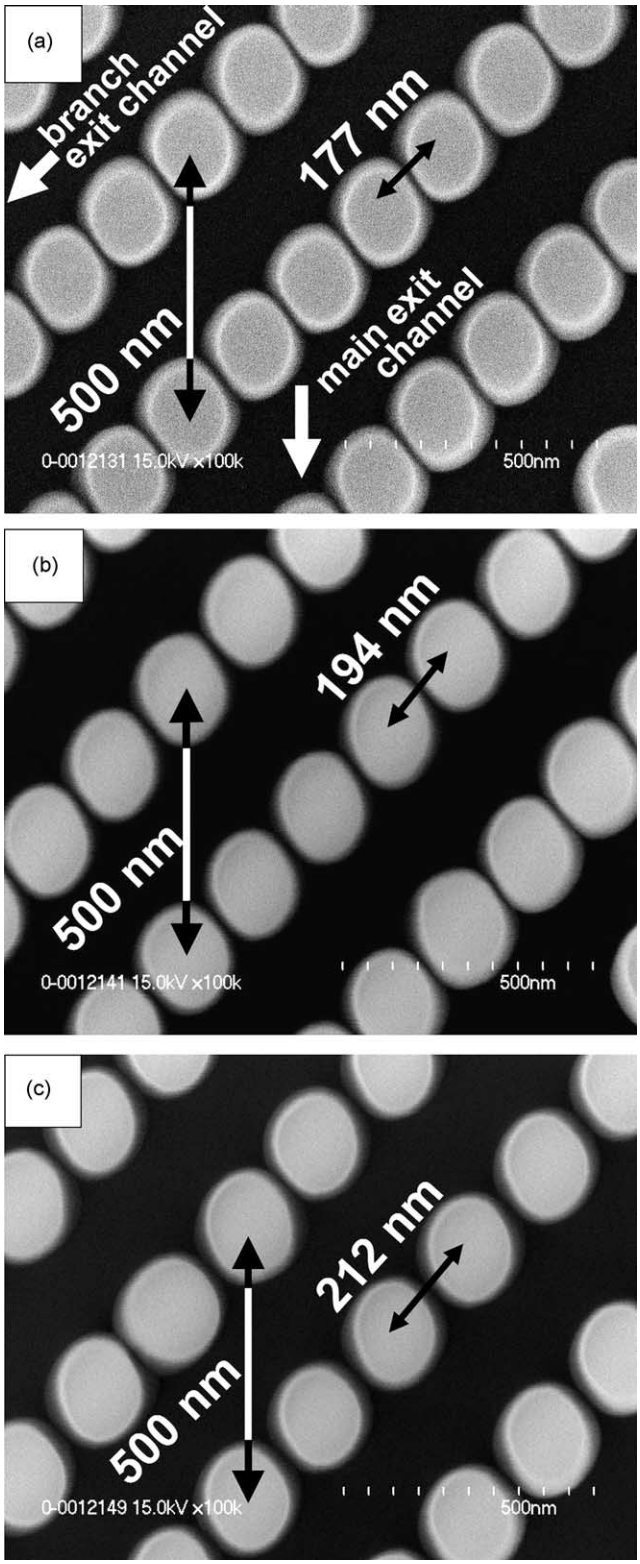

Fig. 4. Enlarged scanning electron micrographs of nano-pillar anisotropic arrays at junction exit to main exit channel. Intervals between nano-pillars vary with directions. Constant interval between all nano-pillars in direction of main exit channel is 500 nm. (a) Chip A: interval in direction of main exit channel is 177 nm. (b) Chip B: interval is 194 nm. (c) Chip C: interval is 212 nm.

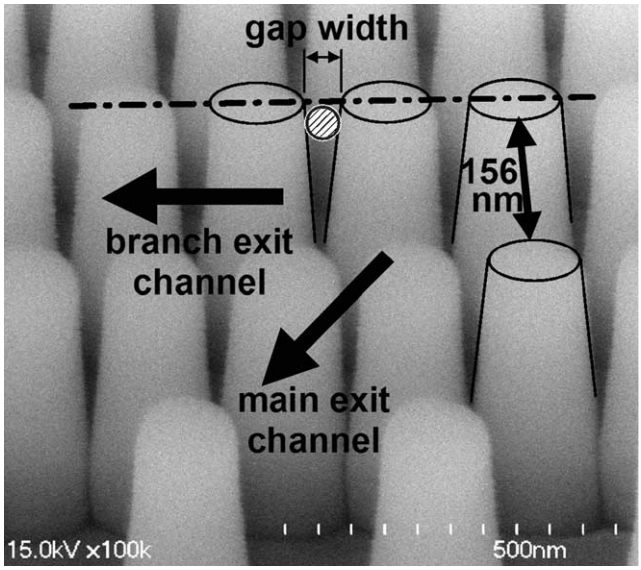

Fig. 5. Scanning electron micrograph of oblique-perspective view of nano-pillar array on chip B observed downward at an angle of 45°. Maximum diameters of particles illustrated with circle, which can pass through the gap, were estimated from this view.

channel in respective observations. Then, −5 V was applied to the reservoir electrode at the inlet, 18 V to the one at the main channel outlet, and 1.5 V to the one at the branch channel outlet. The layouts for the main and branch exit channels were designed so that the electric fields at the junction towards the main and branch exit channels were almost in proportion to the reservoir voltages. Consequently, the electric field to the main exit channel was set higher than that to the branch exit channel.

4. Results and discussion

Fig. 6 shows micrographs at the junction of chip A taken with a charge-coupled device camera mounted on a fluorescent microscope. The white luminescent spots correspond to fluorescently stained DNA molecules.

As shown in Fig. 6a, since 300 base pair (bp) DNA fragments with an estimated gyration diameter of 57 nm [11], could not pass through the 32-nm-wide gap opening to the main exit channel, most of these flowed to the outlet of the branch exit channel. The electrophoretic flow of 100 bp (22 nm in diameter) fragments is shown in Fig. 6b. In this case, the diameter is smaller than the width of 32 nm of the narrow gap opening to the main exit channel. Therefore, these fragments can pass through the both gaps opening to the main and branch exit channels. Then, these fragments drifted and dispersed in bi-forked junction according to both of the electric field and the obstruction by the nano-pillars. Finally, most of the fragments flowed along the main exit channel due to the higher electric field driving them to the outlet of the main exit channel. There were such small quantities of

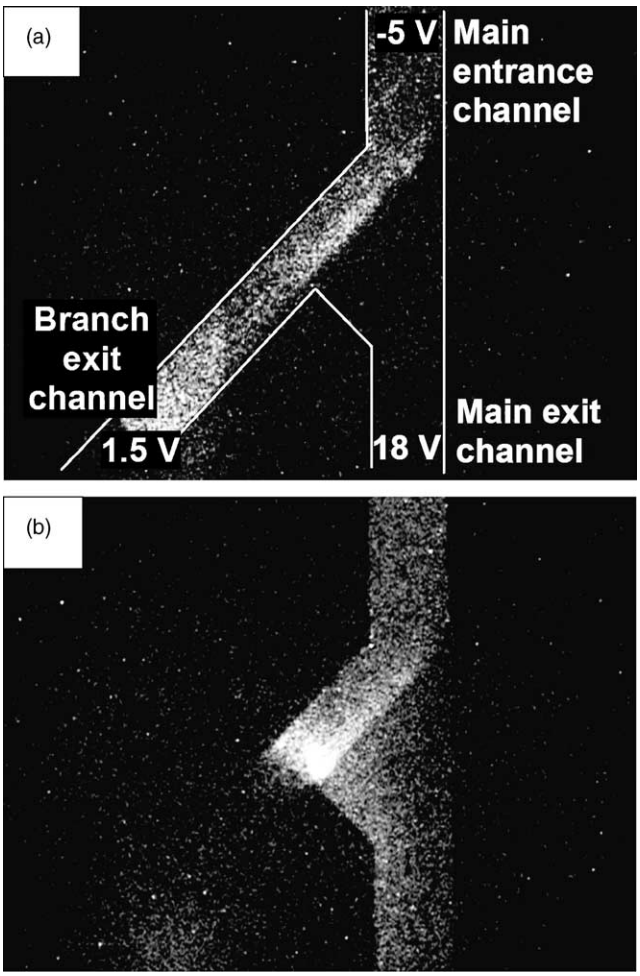

Fig. 6. Micrographs at junction of chip A taken with a charge-coupled device camera mounted on fluorescent microscope. White luminescent spots in channels reveal DNA molecules fluorescently stained with YOYO-1, which are electrophoresed. Applied voltages were −5 V to inlet, 18 V to outlet of main channel, and 1.5 V to outlet of branch channel. (a) Three hundred base pairs DNA fragments (57 nm in diameter). Channel indicated by white solid lines. (b) One hundred base pairs DNA fragments (22 nm in diameter).

DNA fragments, which flowed to the outlet of the branch exit channel, that they could hardly be observed. These results indicate that the anisotropic array of nano-pillars controlled the flow direction of these DNA molecules according to their sizes under the same electric fields. The fluorescent DNA fragments in Fig. 6a were widely dispersed across the branch exit channel. This indicates that the two-dimensional array of the gaps effectively prevented macromolecules from gathering in a line on mesh with specific gap widths.

Fig. 7 illustrates the dependence of DNA size on the direction of the electrophoretic flow evaluated using chips A, B, and C. In this figure, the *x*- and *y*-axes indicate the gap widths and diameters of DNA fragments. The closed circles indicate in which most DNA fragments flowed to the main exit channels and the open squares indicate those for the branch exit channels. On each gap width of 32, 52, and 70 nm, smaller and larger DNA fragments tend to flow to the

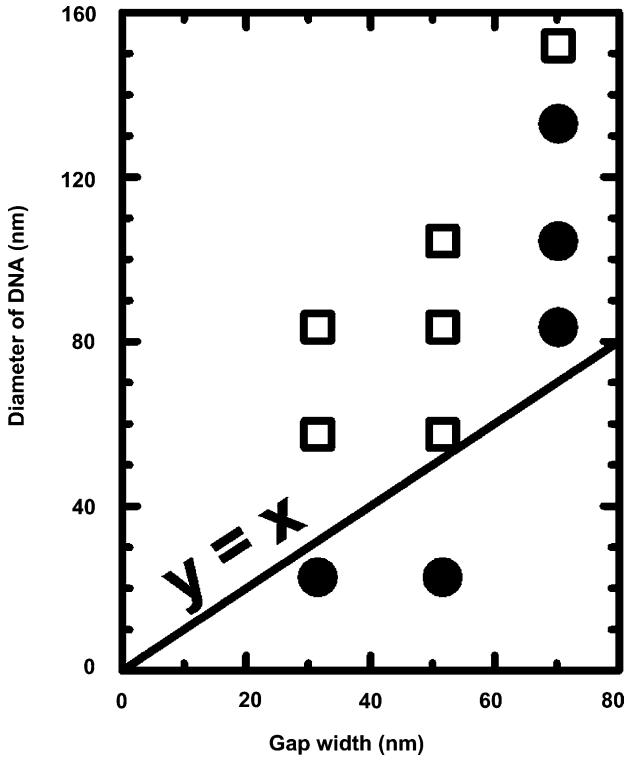

Fig. 7. Dependence of DNA size on direction of electrophoretic flow. Closed circles indicate direction where most DNA fragments flowed to main exit channel and open squares indicate where most flowed to branch exit channel. Solid line plots where DNA diameter equals to gap width.

main and the branch exit channels. This means that controlling the direction of flow with anisotropic nano-pillar arrays was successfully demonstrated in all chips. Whether DNA fragments could pass through the gap was determined in relation to their diameters and the gap width of the mesh. In addition, the nanometer-scale gap width is much smaller than micrometer-scale diffusion lengths caused by Brownian motion. Consequently, this flow direction control operated according to a simple sieving principle, not the diffusion principle with Chou et al.'s chip.

The relation for the diameter of DNA equaling the gap width is plotted with the solid line in Fig. 7. It runs between the closed circles and open squares at the both gap widths of 32 and 52 nm. This indicates that DNA fragments with the diameters of 22 and 57 nm, which are close to these gap widths, behaved as rigid spheres in this experimental accuracy. However, the boundary at a gap width of 70 nm between the closed circles and open square is higher than the solid line. This suggests that the larger DNA fragments tend to deform more easily to thinner shapes and to pass through the gaps. A similar tendency is generally discussed using the relation between rigidity and sizes of DNA fragments [11]. Consequently, the DNA fragments with a diameter of 57 nm or smaller tended to be rigid, and those that were 83 nm or larger tended to be flexible under these experimental conditions. Therefore, this flexibility needs to be considered in chip design for fractionating DNA fragments.

5. Conclusion

We proposed a size-based pre-fractionation chip in this paper with continuous-flow fractionation units that could be applied to enrich macromolecules of interest. These fractionation units had nano-pillar anisotropic arrays that functioned as sieve meshes. In contrast to conventional size-based pre-fractionation by column chromatography, these fractionation units provided continuous-flow operation without dilution. This continuous-flow operation eliminated the limitations with sample loading volume. Additionally, the small channel-volume, which is characteristic of chip-based systems could reduce sample loss.

To prove the effectiveness of conceptual chip design and its operating principles, we fabricated chips with continuous-flow fractionation units using nanometer-scale fabrication technology. Gap widths close to the diameters of macromolecules were achieved in these chips, which controlled the flow direction of electrophoretic DNA molecules according to their sizes. This indicated that operation was based on the sieving principle. In contrast to the diffusion operation, this sieving operation did not involve a statistical spreading factor for fractional resolution. Therefore, low cross contamination between the fractionated samples could be expected in comparison with other chips, whose operation was based on the diffusion principle. Furthermore, because sieving operation was not limited to a combination of DNA molecules and electrophoresis, these types of size-based pre-fractionation chips could be applied to a combination of various kinds of macromolecules and driving forces.

References

[1] P.G. Righetti, A. Castagna, B. Herbert, F. Reymond, J. Rossier, Proteomics 3 (2003) 1397.
[2] M.M. Shaw, B.M. Riederer, Proteomics 3 (2003) 1408.
[3] D.E. Garfin, Trends Anal. Chem. 22 (2003) 263.
[4] S.C. Jacobson, J.M. Ramsey, in: M.G. Khaledi (Ed.), High Performance Capillary Electrophoresis, Wiley, New York, 1998, p. 613.
[5] M. Baba, T. Sano, N. Iguchi, K. Iida, T. Sakamoto, H. Kawaura, Appl. Phys. Lett. 83 (2003) 1468.
[6] N. Kaji, Y. Tezuka, Y. Takamura, M. Ueda, T. Nishimoto, H. Nakanishi, Y. Horiike, Y. Baba, Anal. Chem. 76 (2004) 15.
[7] C. Chou, O. Bakajin, S.W.P. Turner, T.A.J. Duke, S.S. Chan, E.C. Cox, H.G. Craighead, R.H. Austin, Proc. Nat. Acad. Sci. U.S.A. 96 (1999) 13762.
[8] C. Chou, R.H. Austin, O. Bakajin, J.O. Tegenfeldt, J.A. Castelino, S.S. Chan, E.C. Cox, H. Craighead, N. Darnton, T. Duke, J. Han, S. Turner, Electrophoresis 21 (2000) 81.
[9] J. Fujita, Y. Ohnishi, Y. Ochiai, S. Matsui, Appl. Phys. Lett. 68 (1996) 1297.
[10] T. Sano, N. Iguchi, K. Iiida, T. Sakamoto, M. Baba, H. Kawaura, Appl. Phys. Lett. 83 (2003) 4438.
[11] J.L. Viovy, C. Heller, in: P.G. Righetti (Ed.), Capillary Electrophoresis in Analytical Biotechnology, CRC Press, Boca Raton, FL, 1996, p. 480.